ECCOMAS Congress 2016
VII European Congress on Computational Methods in Applied Sciences and Engineering
M. Papadrakakis, V. Papadopoulos, G. Stefanou, V. Plevris (eds.)
Crete Island, Greece, 5–10 June 2016

SEISMIC ASSESSMENT OF MASONRY ROCKING COLUMNS AND FRAMES UNDER GROUND MOTION EXCITATIONS

Ioannis E. Kavvadias[1], **Lazaros K. Vasiliadis**[1]

[1] Democritus University of Thrace, Dept. of Civil Engineering
Vas. Sofias 12, 67100 Xanthi, Greece
e-mail: {ikavvadi, lvasilia}@civil.duth.gr

Keywords: Ancient Columns, Rocking Columns; Rocking Frames, Ground Motion Intensity Measures, Fragility Curves, Earthquake Engineering.

Abstract. *In this study the seismic response of free standing, rocking columns and frames is investigated taking into account different intensity measures (IMs) of the seismic excitations. The seismic vulnerability of the examined structural systems is based on the probabilistic seismic demand model (PSDM), in which the degree of uncertainty is depended on the IM used. Thus 23 different IMs are evaluated in order to extract the most optimal one. A performance based analysis is performed and fragility curves are generated conditional on uni-variable and bi-variable IMs considering the maximum rotation normalized to the slenderness as engineering demand parameter (EDP). The seismic assessment of these structures is evaluated using three limit states. Nevertheless, in this study, the effect of the beams' mass on the seismic rocking behavior of the frames is also examined. Finite element analysis models are used for the simulation of the structural members as deformable bodies while rigid contact elements are employed for the interfaces. Time domain analyses are performed using a set of 30 natural ground motions. Results in terms of correlation coefficients and dispersion values are first presented, indicated that the length scale of the excitation (Lm) and the vector value IM, PGV-Tm are the most optimal uni-variable and bi-variable IMs, for describing the rocking response. Further results in terms of peak rocking rotations and fragility curves shown that free standing frames are less vulnerable than the single columns. Moreover, as the beam mass increases, the developed rocking rotation of the frame tends to be reduced.*

1 INTRODUCTION

The investigation of the seismic response of ancient structural systems such as ancient columns and colonnades has received increasing attention during the last decades. These structural systems comprise the construction technique of Archaic, Classical, and Roman temples. Different types of columns with numerous variations in their geometrical characteristics can be found mainly in the Eastern Mediterranean region. In general, ancient columns are earthquake resistant, as proven from the fact that many monuments like these have survived many strong earthquakes over the centuries. This notable stability is displayed mainly due to the design method of these structures which is based on articulated mechanisms that demonstrate rocking behavior. Usually these are constructed of limestone or marble blocks (drums), which are placed on top of each other, without connecting mortar between them. These rigid-body assemblies display a very different dynamic response compared to modern structures. Their main difference as shown in Figure 1 is that the rocking behavior exhibits negative stiffness and low damping that occur only at the instant of impact in contrast with the modern design philosophy which is based on the positive stiffness of the structure and the ductility of the structural members [1]. Their response is composed primarily of rocking and sliding among the individual blocks of the structure and the ground. This behavior can be characterized as highly nonlinear due to the continuous changing of geometry and boundary conditions of the structural system during a strong earthquake.

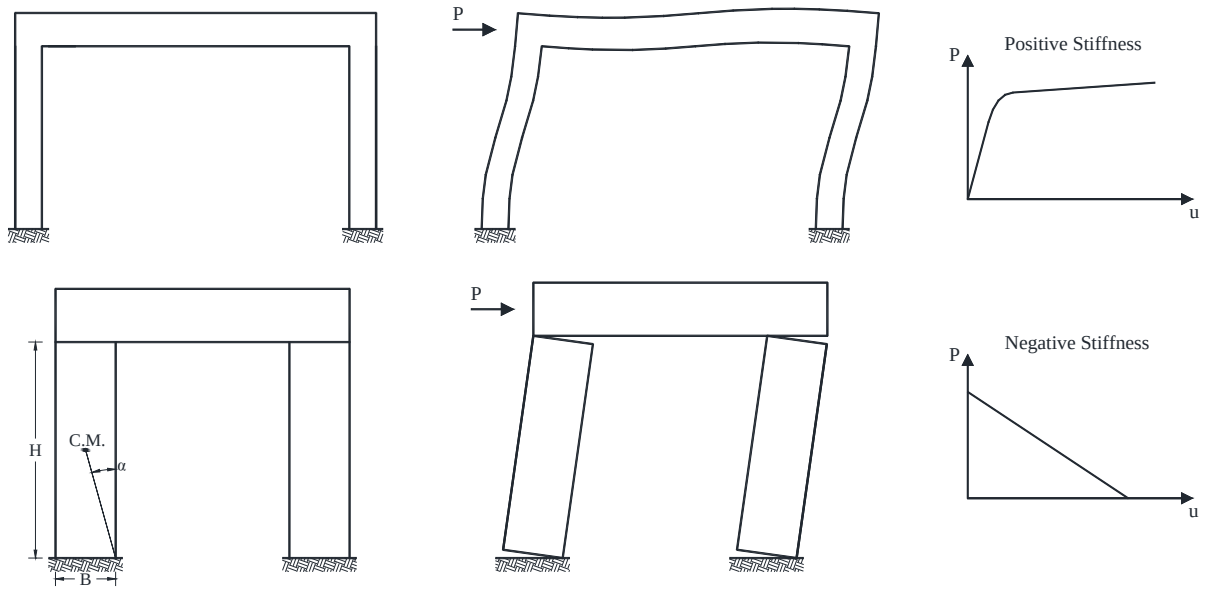

Figure 1: Response of a moment resistance frame versus a rocking frame.

Early work on the dynamics of the rocking column started analytically by Milne (1885) [2] while, Omori (1990) [3] was one of the first who performed experimental research on the seismic response of rectangular rocking columns. Subsequently, Kirkpatrick (1927) [4] presented a novel paper in which he relates the column size and the period of the excitation with the rocking response. It was Housner's (1963) [5] study that offers a solution for the dynamic behavior of a single block under pulse excitation, through the formulation of the inverted pendulum. Housner revealed both the size effect, which means that the larger block between two with the same aspect ratio exhibits greater stability under horizontal excitation, and the frequency effect which indicates that the frequency content of the excitation substantially affects

the rocking response, with long period excitations being more likely in causing overturning than the short period ones. His pioneer work constitutes the basis of the rocking analysis theory. After these studies several followed as researchers were motivated by the need to understand the rocking response, and they extended our previous knowledge, by revealing hidden aspects of rocking response [6-13].

Multi block rocking response has also been under investigation [14-18]. Sinopoli's work [14] has examined the impact problem between rigid bodies through a kinematic approach. Meanwhile, Psycharis [15] and subsequently Spanos et al. [16] proposed analytical solutions for the rocking response of two stacked rigid blocks assuming no sliding between them. Furthermore, Makris and Vassiliou [17] present the equivalence between a rocking frame and singular rocking blocks whereas, DeJong and Dimitrakopoulos [18] generalized it also for asymmetric rocking frames.

Extensive numerical investigation specifically on the response of ancient structural systems such as free standing single monolithic and multi-drum columns or columns connected to each other at the top level by architraves, which are usually consist the peristyles of ancient temples, has been presented by several researchers [19-25]. The numerical modeling of all these studies has been conducted using the Discrete Element Method (DEM). Using planar numerical modeling Psycharis et al. [19] investigated the seismic response of ancient columns. Moreover, Konstantinidis and Makris [20] also using a two dimension modeling, examined the effect of wooden poles installed in ancient times, but also of titanium poles which were installed during the restoration process, on the dynamic response of multidrum columns. Additionally, studies are presented on the seismic response of ancient columns and colonnades with epistyles using a custom-made software based on the DEM [23], [24]. On the other hand, Papantonopoulos et al. [21] and Psycharis et al. [22] performed numerical analyses in three dimensions. It was noticed that 2D analyses are capable of capturing the rocking phenomenon but without computing the out of plane oscillation, which makes the problem more complex. Thus is slightly underestimate the overall response. Experimental studies were also performed by Mouzakis et al. [26] Pena et al. [27] and Drosos and Anastopoulos [28] and confirmed the conclusion obtained from the numerical studies.

Due to the sensitivity of rocking response even to trivial changes of the ground motion characteristics or of the geometry of the model, Spanos and Koh [29] were the first to study the rocking response via a probabilistic framework. Afterwards, seismic vulnerability assessment of rocking columns and frames were presented by Psycharis et al. [30] and Dimitrakopoulos and Paraskeva [31].

In this paper, we present a numerical investigation of the seismic response of free standing columns and colonnades. Time domain analyses are performed with the use of 30 natural records. The scope of this study is to assess the seismic vulnerability of the examined rocking structures resulting in the most optimal intensity measures (IMs) [32] used for generating the probabilistic seismic demand model [33]. In addition, the difference of the colonnade with epistyle behavior against the single column response is studied while, the influence of the beams' mass on the rocking response is also examined.

2 NUMERICAL MODELING

For the purpose of this study, finite element models are utilized for the in space simulation of the members, in which the blocks are simulated as deformable elements and the ground as a rigid surface. Despite the structural members being modeled as 3D members, planar analyses were performed. Explicit dynamic analyses were employed as it is computationally efficient for discontinuous events like impact problems, using the central difference algorithm. Of particular significance for the simulation are the appropriate modeling of the contact between

the blocks and the base, and in the case of multi block models the contact between each block. Rigid contact is used to model the interfaces while a Mohr-Coulomb model is adopted to describe the mechanical behavior of the joints. For both normal and tangential direction of the contact element, the stiffness is assumed as infinite. In the normal direction no tensile strength is considered while the shear strength is governed by the Coulomb friction coefficient without considering cohesion. As mentioned by a thorough investigation made by Papantonopoulos et al. [21], damping affects the amplitude of the intense rocking response and thus, zero value of damping gives better results during the strong motion part of the excitation. Consequently both the mass proportional damping and the stiffness proportional damping coefficients are set zero for the analyses. The mechanical properties of the block material as well as the interface properties listed in Table 1 are assumed as typical values for marble blocks.

Material Properties	Density (kg/m^3)	2750
	Young's modulus (Gpa/m)	84.5
	Poison ratio	0.23
Interface Properties	Friction coefficient	0.70
	Cohesion (MPa)	0
	Tensile strength (MPa)	0

Table 1: Material and interface mechanical properties.

Column with 8m height and slenderness α=0.165rad is studied. The selection of the dimension was made to be in accordance with the size and the slenderness of recorded ancient columns. Specifically the columns of the Temple of Olympic Zeus and the Temple of Apollo in Syracuse have 8 m height. Additionally the Parthenon Pronaos columns have a slenderness of 0.16rad. Concerning the effect of the architrave existence, two varying geometry architraves are examined. The values of the beam (architrave) mass (m_b) are defined as a ratio over the columns mass (m_c), taking values $m_b/2m_c$=0.25, 0.5. The axial distance between the columns is 3m and is spanned with a single block architrave. Figure 2 shows the dimensions in meters of the examined rocking column and frames.

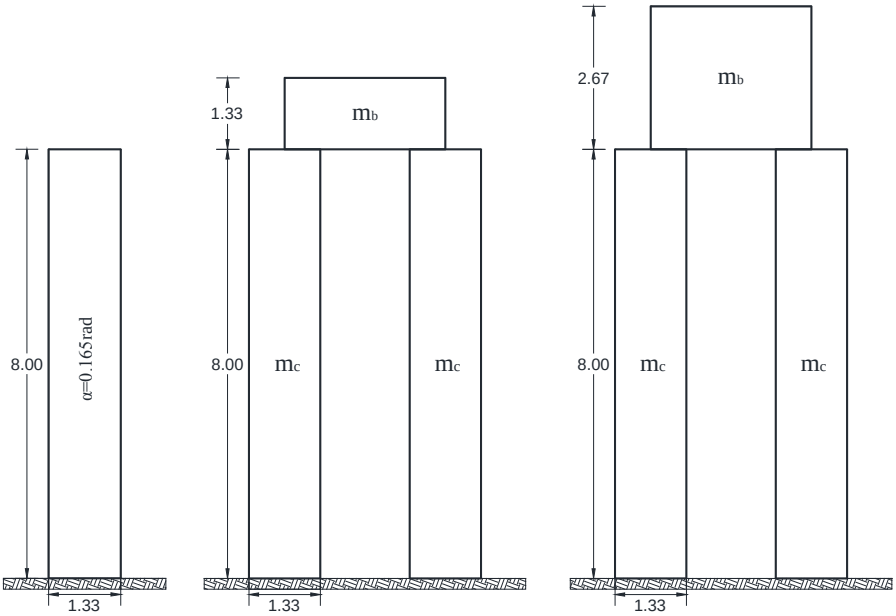

Figure 2: Examined cases of free standing column and free standing frames.

3 SELECTION OF NATURAL GROUND MOTIONS AND INTENSITY MEASURES (IMS)

3.1 Ground Motions

A set of 30 ground motion time histories is used as input ground motion for the analyses. What proved to be useful, for the selection was an extensive review of ground motion selection methods for dynamic analysis of structural systems presented by Katsanos et al. [34]. The events were chosen from worldwide well-known sites with strong seismic activity. Excitations generated from different types of fault types, with earthquake magnitudes (M_s) between 5.3 and 7.6, including both near fault and far fault records as the closest distance to fault rapture (R) varying from 0.6 to 115 km is employed in order to present a wide range of intensities and frequency contents. A further aspect which has been taken into consideration is the expected damage potential of the seismic excitation on the structure. Seismic excitations which provide a wide spectrum of structural damage, from negligible to severe, are taken into account. Based on the above assumption, a rigorous selection of ground motions carried out from the PEER [35] and the European [36] strong motion databases in order to use original records without any scaling. The complete list of the natural ground motions used for the analyses is shown in Table 2.

Earthquake	Record	Date	M_s	R (km)
Aigion	AIGA	25/06/1995	6.4	21.5
Athens	ATH4	07/09/1999	5.90	16.62
Bucharest	Bucharest	04/03/1977	7.50	115.0
Chi-Chi	CHY035	20/09/1999	7.62	12.56
Chi-Chi	TCU88	20/09/1999	7.62	18.16
Chuetsuoki	Nakanoshima Nagaoka	16/07/2007	6.8	19.89
Coalinga	Fault Zone 14	02/05/1983	6.36	29.48
Corinth	Corinth	24/02/1981	6.60	10.28
Darfield	Papanui High School	04/09/2010	7	26.76
Duzce	Lamont 531	12/11/1999	7.14	8.03
Erzincan	Erzincan	19/03/1992	6.69	4.38
Friuli	Tolmezo	06/05/1976	6.50	15.82
Gazli	Karakyr	17/05/1976	6.80	5.46
Imperial Valley	El Centro Array #9	19/05/1940	6.95	6.09
Imperial Valley	El Centro Array #7	15/02/1979	6.53	0.56
Imperial Valley	El Centro Array #8	15/02/1979	6.53	3.86
Irpinia	Sturno	23/11/1980	6.9	10.84
Iwake	Ichinoseki Maikawa	14/07/2008	6.9	23.02
Kalamata	Kalamata	13/09/1986	6.20	10.00
Kobe	Nishi -Akashi	16/01/1995	6.90	7.08
Kobe	Takatori	16/01/1995	6.90	1.47
Landers	Joshua Tree	28/06/1992	7.28	11.03
Loma Prietta	Los Gatos - Lexington Dam	17/11/1986	6.93	5.02
Northridge	Paicoma Dam	17/01/1994	6.69	7.01
Parkfield	Cholame #2	28/06/1966	6.20	17.64
San Fernando	Paicoma Dam	09/02/1970	6.61	1.81
Taiwan SMART1(40)	Smart1 M02	15/111986	6.32	60.89
Superstition Hill	Mtn Camera	24/11/1987	6.54	5.61
Tabas	Dayhook	16/09/1978	7.35	13.94
Whittier	LA - Obregon Park	01/10/1987	5.27	13.62

Table 2: List of the ground motions used in this study.

3.2 Intensity measures (IMs)

In order to designate the optimal earthquake intensity measures (IMs) for rocking response, a large number of seismic parameters is considered in the present study. Specifically 25 IMs were taken into account which can be classified into time history, energy, spectral, and frequency parameters. The definition of all the examined IMs is presented by Kramer [37]. Regarding the time history parameters, peak ground acceleration (PGA), peak ground velocity (PGV), peak ground displacement (PGD), sustain maximum acceleration (SMA), sustain maximum acceleration (SMV), and effective design acceleration (EDA) are taken under consideration. Additionally, with regard to the energy parameters the following were considered, root mean square of acceleration (A_{rms}), of velocity (V_{rms}), and of displacement (D_{rms}), characteristic intensity (I_c), Arias intensity (I_α), cumulative absolute velocity (CAV), specific energy density (SED), strong motion duration (T_D) and Fajfar index (I_F). The examined rocking structures do not possess natural modes in the classical sense [21] and so we do not use as intensity measures, spectral acceleration or velocity values for a certain period, although we consider the acceleration spectrum intensity (ASI), the velocity spectrum intensity (VSI) and the Housner Intensity (SI_H).

According to the frequency parameters, the period corresponding to the peak acceleration ($T_{p,A}$) and to the peak velocity ($T_{p,V}$) of the elastic response spectrum, are of the most extensively used frequency parameters in earthquake engineering. Nevertheless, none of these parameters represent the frequency content of a signal, except for the second one which seems to be a good approach to it. Mean period (T_m) [38] which is calculated by the Fourier spectra seems to be the best frequency parameter for excitations with arbitrary time-history shape. Moreover, the ratio PGV/PGA is related to the frequency content of the excitation, as for a harmonic motion this ratio is equal to $PGV/PGA=T/2\pi$. Finally, the characteristic length scale $L_p=v_p \cdot T_p$, which is introduced by Makris and Black [39] for pulse-type excitations and extended for non-distinct pulses by Dimitrakopoulos et al. [40], is considered too.

4 FRAGILITY ANALYSIS

4.1 Probabilistic seismic demand model

The vulnerability is assessed by estimating the conditional probability P where the seismic demand D measured to a specific engineering demand parameter (EDP), is higher than its capacity C, for a given value of a ground motion IM.

$$Fragility = P[D \geq C \,|\, IM] \tag{1}$$

The capacity is estimated by the proposed limit states while the demand is estimated using the relationship between the median structural demand Sd and each IM [33]:

$$S_d = aIM^b \tag{2}$$

where α and b are the linear regression coefficients for the logarithmic expression of the assumed scale law.

Assuming lognormal distribution for both the demand and the capacity of the structure and considering only demand uncertainties ($\beta_{D|IM}$), equation (1) can be rewritten in the following form:

$$P[D \geq C \,|\, IM] = \Phi\left(\frac{\ln(S_d / S_c)}{\sqrt{\beta_{D|IM}{}^2}}\right) \tag{3}$$

where Φ is the standard normal cumulative distribution function, Sc is the median value of the capacity which is estimated through the adopted limit states and $\beta_{D|IM}$ is the dispersion or logarithmic standard deviation for the demand conditioned the IM. For the calculation of the conditional standard deviation of the regression which is used to estimate the desperation, the following equation is utilized, where di is the i-th realization of the demands from the time history analyses.

$$\beta_{D|IM} \cong \sqrt{\frac{\sum(\ln(d_i) - \ln(aIM^b))^2}{N-2}} \tag{4}$$

In order to conclude in an intensity measure that could reduce even more the demand uncertainty ($\beta_{D|IM}$), also is examined vector IMs (couple of IMs) [41] to express the median demand as defined in the follow equation:

$$S_d = aIM_1^{b_1} IM_2^{b_2} \tag{5}$$

4.2 Definition of the engineering demand parameter

The introduced engineering demand parameter (EDP) has to get a clear physical meaning. Being aware of this principal, for the examined free standing structures, the best EDP that can be used has to be based on the rocking rotation as rocking is the dominant response of this structure. The absolute maximum developed rotation $|\theta_{max}|$ divided to the critical overturning rotation which is equal to the slenderness of the column α, was selected.

$$EDP = \frac{|\theta_{max}|}{\alpha} \tag{6}$$

4.3 Definition of the proposed limit states

Performance Based Earthquake Engineering has introduced the concept of acceptable performance levels. In vulnerability assessment analysis, capacity limit states (LS) are required to be defined, since the objective of the fragility analysis is to obtain the probability of exceedance the stated performance criteria. The capacity should be measured with the metrics of the EDP. Three performance levels, as presented in Table 3 are proposed for the current study. The first limit state (LS_I) corresponds to slight rocking of the structure, the second (LS_{II}) to moderate rocking which may cause local damage (imperfections) due to the impact and finally the third (LS_{III}) that corresponds to collapse due to rocking overturn.

Limit State	$\|\theta_{max}\|/\alpha$	Performance Level	Description
LS_I	0.20	Damage limitation	Lightly damaged structure.
LS_{II}	0.40	Moderate Damage	High likelihood of local damage due to impact.
LS_{III}	1.00	Near collapse	Rocking overturn of the structure.

Table 3: Proposed performance criteria.

5 RESULTS

5.1 Correlation analysis

To estimate the grade of interdependency between the intensity measures and the rocking response, the correlation coefficient according to Pearson is calculated. Pearson correlation coefficient shows how well the data fit to a linear relationship. The variables relationship is

based on the scale law of Equation (2). Figure 3 presents the correlation coefficient between the IMs and the EDP for the cases of a the free standing column and the free standing frame with masses ratio $m_b/2m_c=1/4$.

Examining Spearman's rank correlation coefficient of Figure 3, the maximum correlation of the adopted EDP with all the velocity based ground motion parameters is easily reconcilable. Specifically PGV and I_F is the IMs that has the strongest correlation with the EDP followed by the response spectrum IM SI_H. In addition, it is noted that the developed rocking rotation is influenced by the frequency parameters. The mean period of the excitation (T_m) and the ratio PGV/PGA exhibit the highest grade of interdependency, whereas between the predominant periods of the acceleration and the velocity elastic response spectrum, the second one has a higher value of correlation with the EDP. Finally the characteristic length scale of the excitation (L_m) displayed the strongest correlation among all the IMs.

On the other hand, the acceleration based parameters present the lowest grade of interrelationship with the rocking behavior. Additionally, the displacement based as the duration IMs show very low correlation levels with the EDP. Among the IMs which least affects the rocking behavior are the PGA the SMA and the TD.

From the results of the correlation analysis it can be concluded that the IMs associated with the velocity and the frequency content of the ground motion exhibit a far better correlation with the examined EDP. On the contrary, the IMs associated with the acceleration, the displacement and the duration of the excitation exhibit the lowest interdependency with the rocking rotation.

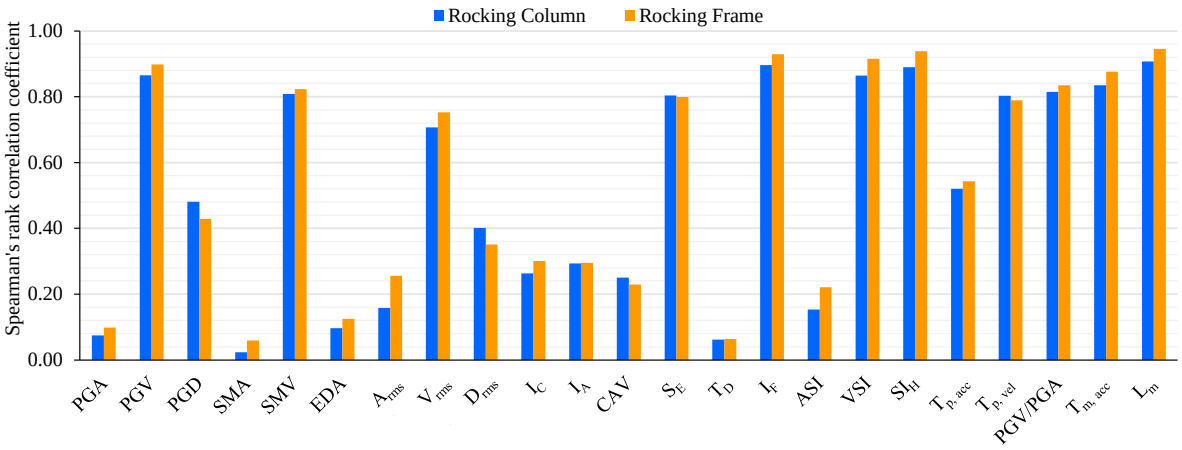

Figure 3: Correlation coefficients between the intensity measures and the engineering demand parameter.

5.2 Median seismic demand

The median demand models are generated from the linear regression analyses. Table 4 summarizes the expression of the median, the regression coefficient R^2 and the dispersion $\beta_{D|IM}$ of the seismic demand conditioned on a certain IM, for the cases of the free standing column. One of the main objectives of this paper is to estimate the most appropriate IM that reduces the uncertainty in the seismic demand model of rocking structures. The most efficient IMs are those that decrease the amount of the variation in the estimated median demand which means reduced uncertainty.

IM	PSDM	R^2	$\beta_{D\|IM}$
PGA	ln(0.202) + 0.256ln(IM)	0.01	1.31
PGV	ln(2E-4) + 1.729ln(IM)	**0.75**	**0.66**
PGD	ln(0.035) + 0.538ln(IM)	0.23	1.15
SMA	ln(0.172) + 0.072ln(IM)	0.01	1.31
SMV	ln(0.001) + 1.633ln(IM)	0.65	0.77
EDA	ln(0.219) + 0.331ln(IM)	0.01	1.30
A_{rms}	ln(0.803) + 0541ln(IM)	0.03	1.29
V_{rms}	ln(0.015) + 1.264ln(IM)	0.50	0.93
D_{rms}	ln(0.090) + 0.389ln(IM)	0.16	1.20
I_c	ln(1.010) + 0.68l3n(IM)	0.07	1.26
I_A	ln(0.133) + 0.549ln(IM)	0.09	1.25
CAV	ln(0.002) + 0.651ln(IM)	0.06	1.27
S_E	ln(0.001) + 0.755ln(IM)	0.65	0.78
T_D	ln(0.117) + 0.124ln(IM)	0.01	1.31
I_F	ln(8E-05) + 1.820ln(IM)	**0.80**	**0.58**
ASI	ln(0.289) + 0.475ln(IM)	0.02	1.30
VSI	ln(3E-05) + 1.761ln(IM)	0.75	0.66
SI_H	ln(1E-04) + 1.541ln(IM)	0.79	0.60
$T_{p,\,acc}$	ln(0.383) + 0.896ln(IM)	0.27	1.12
$T_{p,\,vel}$	ln(0.209) + 1.388ln(IM)	0.65	0.78
PGV/PGA	ln(5.759) + 1.619ln(IM)	0.67	0.76
$T_{m,\,acc}$	ln(0.419) + 1.688ln(IM)	**0.70**	**0.72**
$L_{m,\,acc}$	ln(0.008) + 0.984ln(IM)	**0.82**	**0.55**

Table 4: Seismic demands model for the examined IMs.

It is noted that as the coefficient of determination R2 reaches higher values, the dispersion $\beta_{D|IM}$ gets less. Indicated also from the correlation analysis the IMs that minimize the variation of the data in the median demand model, being in general, the velocity and the frequency based ground motion parameters. Specifically, as the performance of the IMs is evaluated regarding the reduction of the dispersion, the most efficient IMs are the PGV, the I_F, the T_m, and the Lm with dispersion values 0.66, 0.58, 0.72 and 0.55 respectively.

In order to achieve an even better intensity measure from the perspective of efficiency, we lead to examine also vector valued IMs. In this case a multilinear regression analysis was carried out (Equation (5)) in order to minimize the dispersion on the median demand model. Among all the probable IMs combinations, the couple PGV-T_m tends to be the best vector valued IM. The specific IM is generated from the combination of two individual IMs that are not directly interrelated, as the first one is an amplitude parameter and the second one a frequency ground motion parameter. The regression coefficients took values α=0.01, β_1=1.10 and β_2=0.85, the determination coefficient R^2=0.83 and the dispersion $\beta_{D|IM}$=0.54. In comparison with all the single IM models, the standard deviation has been reduced to the bi-variable one. Thus, the efficacy of the multivariable IM is shown in terms of uncertainty reduction.

5.3 Fragility curves

Fragility curves demonstrate the probability that the structure exceeds a certain capacity limit state, given a ground motion intensity level. The fragility curves of the rocking column resulting from the three most optimal IMs are presented in Figure 4.

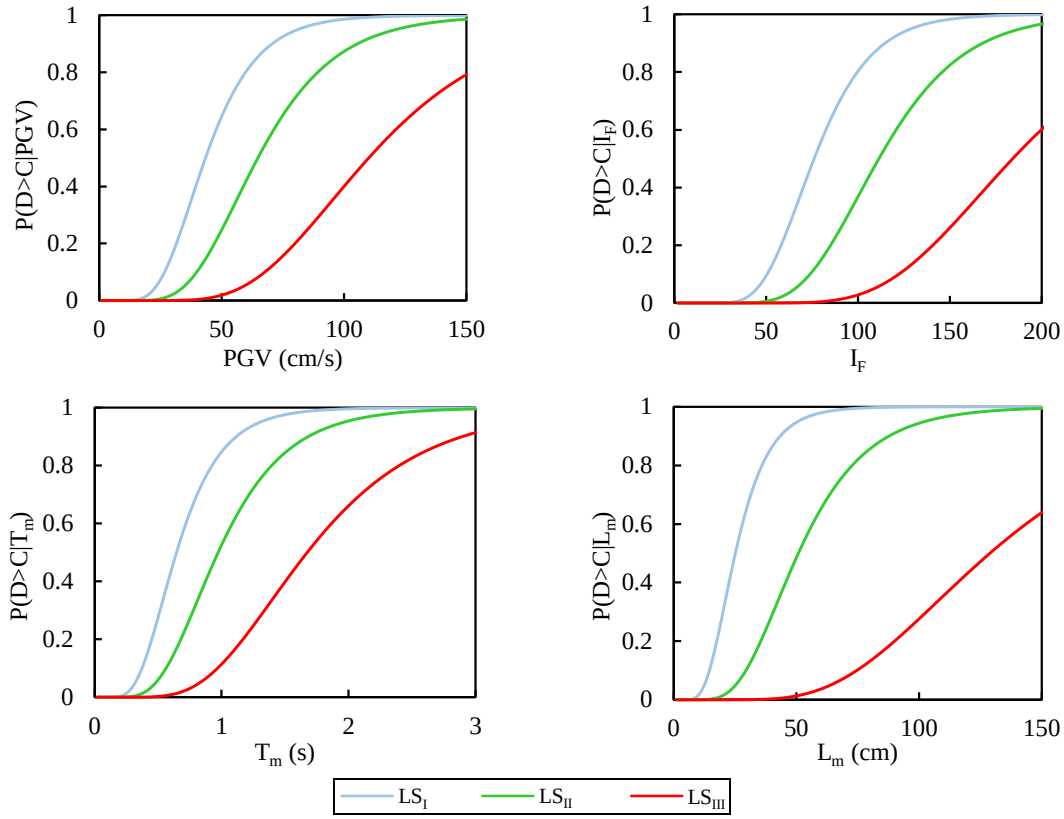

Figure 4: Fragility curves for the three most optimal IMs

The median values of the fragility curves using the PGV for the LS_I, LS_{II}, and LS_{III} are 43, 65 and 110 cm/s respectively whilst, for Farjfar index are 76, 112 and 184 cm/($s^{0.75}$). Using the T_m are 0.64, 0.98 and 1.68 s for the three limit states, and finally using the L_m as intensity measure, the median values of the fragility curves are 25, 51 and 129 cm for each limit state.

It is known that rocking structures exhibit an increased stability. This can also be observed from the fragility curves where the probability of exceeding the LS_{III} which corresponds to collapse by rocking overturn, are limited for intensity measure values that correspond to the majority of the ground motions. However, these structures which constitute some of the world's cultural heritage, have to be preserved undamaged throughout the years. Thus, if needed, we have to propose protection methods for these structures, in order to be preserved from seismic excitations of any magnitude.

Regarding the vector value IM, Figure 5 (a) depicts the surface fragility for all the limit states whilst, Figure 5 (b) shows the fragility curves of exceeding the LS_{II}, for the PGV and for the vector-valued IM which is the couple PGV-T_m. Comparing the single-variable with the bi-variable fragility curves for given Tm values, it is easily observed that as the mean period gets larger values, the vulnerability increases. In addition Table 5 lists the probability of exceedance the stated capacity for various pairs of the 2 IMs and for each IM individually. It is obvious that the bi-variable IM provided a more accurate approach on the definition of the structures' fragility as it can be shifted for even every simultaneous change of each of the two examined IMs. Comparing the probability values of Table 5, it can be seen that fragility curves generated using as uni-variable IM the mean period T_m seem to underestimate the probability of exceedance every stated performance level, especially when the mean period take low values.

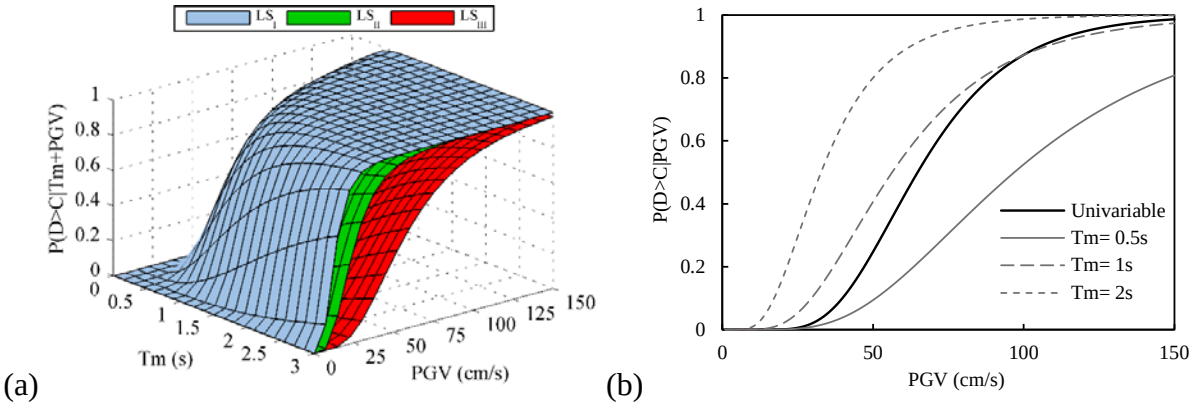

Figure 5: (a) Fragility surfaces using vector-value IM (T_m-PGV), (b) Compative results of univariable with bivariable fragility curves for given values of T_m.

Limit States	Velocity (cm/s)	Mean Period (s)			
		0.5	1	2	univariable
LS1	50	0.48	0.85	0.98	0.65
	100	0.91	0.99	1.00	0.99
	150	0.98	1.00	1.00	1.00
	univariable	0.22	0.85	0.99	-
LS2	50	0.09	0.44	0.80	0.25
	100	0.52	0.87	0.99	0.87
	150	0.81	0.97	1.00	0.98
	univariable	0.06	0.53	0.95	-
LS3	50	0.00	0.28	0.20	0.02
	100	0.05	0.30	0.71	0.40
	150	0.21	0.61	0.91	0.79
	univariable	0.00	0.11	0.66	-

Table 5. Probability values of exceeding the stated performance levels for both univariate and bivariate IMs.

5.4 Mass effect on the rocking response

In this section, the beams' mass effect on the rocking response is examined. The results in terms of peak developed rotation versus the most optimal uni-variable IM, which is the length scale of the excitation (L_m), are presented and compared between the different cases. Subsequently, to obtain results through a vulnerability perspective the fragility curves of exceeding the LS_{II} are displayed (Figure 6).

There are two rocking frames considered with differences of the ratio of the beam mass to the columns masses (Figure 2). From Figure 6 it can be noticed that the single free standing column presents larger values of rocking rotation in contrast with the rocking frames regardless of the rise of the gravity center of the cap beam. Moreover, comparing the seismic response of the frames, the one with the heavier beam exhibits increased stability. Both observations came into agreement with Papaloizou and Komodromos [23] and Makris and Vassiliou [17] conclusions. These remarks can easily be seen from the rotation versus the excitation length scale plot but also from the respective fragility curves.

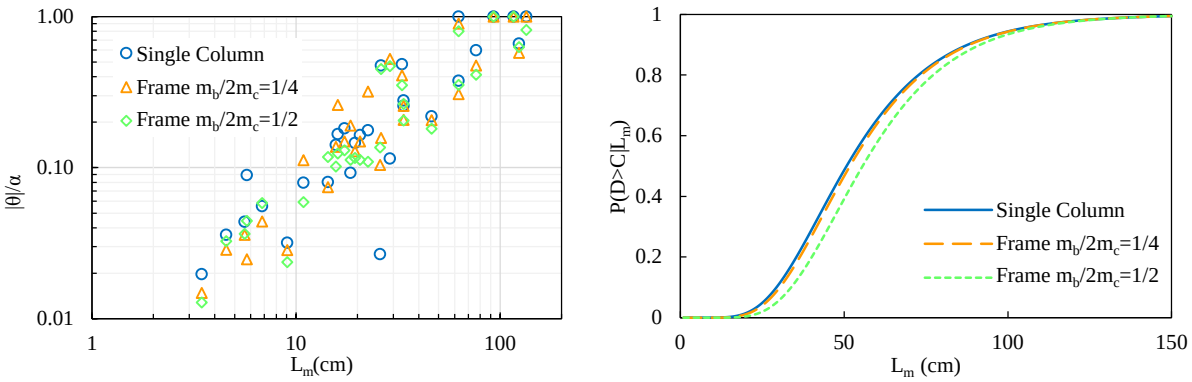

Figure 6: Comparative results of the maximum developed rocking rotation and the fragility curves of exceeding LS_{II}, between a single column and rocking frames with defferent beam masses.

6 CONCLUSIONS

The effect of the seismic excitations parameters on the rocking response of free standing columns and frames is numerically investigated in this paper, in order to conclude in an optimal uni-variable or bi-variable IM that reduces the uncertainties associated with the PSDM. Moreover, the influence of the size and the construction on the response of the structural systems is examined. The conclusion indicated by this study can be summarized as follows:

- Rocking behavior is primarily affected by the velocity based and the frequency content parameters of the ground motion. Specifically, the peak ground velocity (PGV), the Fajfar index (I_F), the mean period (Tm) and the length scale (Lm) of the excitation are the most optimal IMs.
- Vector valued IMs provided better approach on the determination of the fragility curves, than the uni-variable IMs. In addition, between the bi-variables IMs the couple PGV-Tm is the most efficient one.
- Rocking structures exhibit notable stability that can be seen also from the fragility curves in which the probability of overturning due to rocking is limited for IM values, which correspond to the majority of the ground motions.
- Free standing frames are less vulnerable than the single columns. Moreover, as the beam mass increases, the developed rocking rotation of the frame tends to be reduced.

REFERENCES

[1] N. Makris, M. F. Vassiliou, Seismic Response and Stability of the Rocking Frame. *Computational Methods, Seismic Protection, Hybrid Testing and Resilience in Earthquake Engineering*, 249-273, 2015.

[2] J. Milne, Seismic experiments. *Trans. Seismol. Soc. Jpn.*, **8**, 1-82, 1885.

[3] F. Omori, Seismic experiments on the fracturing and overturning of columns. *Publications of the Earthquake Investigation Committee in Foreign Language*, **4**, 69–141, 1900.

[4] P. Kirkpatrick, Seismic measurements by the overthrow of columns. *Bull. Seismol. Soc. Am.*, **17**, 95-109, 1927.

[5] G.W. Housner, The behavior of inverted pendulum structures during earthquakes. *Bulletin of the Seismological Society of America*, **53**, 403-417, 1963.

[6] C. S. Yim, A.K. Chopra, J. Penzien, Rocking response of rigid blocks to earthquakes. *Earthquake Engineering & Structural Dynamics*, **8**(6), 565–587, 1980.

[7] P. D. Spanos, A.S. Koh, Rocking of rigid blocks due to harmonic shaking. *J. Eng. Mech. (ASCE)*, **110**, 1627-1642, 1984.

[8] I. N. Psycharis, P.C. Jennings, Rocking of slender rigid bodies allowed to uplift. *Earthq. Eng. Struct. Dynam.*, **11**, 57-76, 1983.

[9] S.J. Hogan, The many steady state responses of a rigid block under harmonic forcing. *Earthq. Eng. Struct. Dyn.*, **19**, 1057-1071, 1990.

[10] H.W. Shenton, Criteria for initiation of slide, rock, and slide-rock rigid-body modes. J. Eng. Mech. (ASCE), **122**, 690-693, 1996.

[11] N. Makris, Y. Roussos, Rocking response and overturning of equipment under horizontal pulse type motions. *Rep. No. PEER-98/05, Pacific Earthquake Eng. Res. Ctr*. University of California, Berkeley, California, 1998.

[12] A. Pompei, A. Scalia, M.A. Sumbatyan, Dynamics of rigid block due to horizontal ground motion. *J. Eng. Mech. (ASCE)*, **124**, 713-717, 1998.

[13] J. Zhang, N. Makris, Rocking response of free-standing blocks under cycloidal pulses. *Journal of Engineering Mechanics*, **127(**5), 473-483, 2001.

[14] A. Sinopoli, Dynamic analysis of a stone column excited by a sine wave ground motion. *Applied Mechanics Reviews*, **44**(11), 246-255, 1989.

[15] I.N. Psycharis, Dynamic behaviour of rocking two-block assemblies. *Earthq. Eng. Struct. Dynam.*, **19**, 555-575, 1990.

[16] P.D. Spanos, P.C. Roussis, N.P. Politis, Dynamic analysis of stacked rigid blocks. *Soil Dyn. Earthq. Eng.*, **21**, 559-578, 2001.

[17] N. Makris, M.F. Vassiliou, Planar rocking response and stability analysis of an array of free - standing columns capped with a freely supported rigid beam. *Earthquake Engineering & Structural Dynamics*, **42**(3), 431-449, 2013.

[18] M.J. DeJong, E.G. Dimitrakopoulos, Dynamically equivalent rocking structures. *Earthquake Engineering & Structural Dynamics*, **43**, 1543-1563, 2014.

[19] I.N. Psycharis, D.Y. Papastamatiou, A.P. Alexandris, Parametric investigation of the stability of classical columns under harmonic and earthquake excitations. *Earthquake Engineering and Structural Dynamics*, **29**(8), 1093-1109, 2000.

[20] D. Konstantinidis, N. Makris, Seismic response analysis of multidrum classical columns. *Earthquake Engineering and Structural Dynamics*, **34**, 1243-1270. 2005.

[21] C. Papantonopoulos, I.N. Psycharis, D.Y. Papastamatiou, J.V. Lemos, H. Mouzakis, Numerical prediction of the earthquake response of classical columns using the distinct element method. *Earthquake Engineering and Structural Dynamics*, **31**(9), 1699-1717, 2002.

[22] I.N. Psycharis, J.V. Lemos, D.Y. Papastamatiou, C. Zambas, Numerical study of the seismic behaviour or a part of the Parthenon Pronaos. *Earthquake Engineering and Structural Dynamics*, **32**(13), 2063-2084, 2003.

[23] L. Papaloizou, P. Komodromos, Planar investigation of the seismic response of ancient columns and colonnades with epistyles using a custom-made software. *Soil Dynamics and Earthquake Engineering,* **29**, 1437-1454, 2009.

[24] P. Komodromos, L. Papaloizou, P. Polycarpou, Simulation of the response of ancient columns under harmonic and earthquake excitations. *Engineering Structures*, **30**(8), 2154-2164, 2008.

[25] R. Dimitri, L. De Lorenzis, G. Zavarise, Numerical study on the dynamic behavior of masonry columns and arches on buttresses with the discrete element method. *Engineering Structures*, **33**, 3172-3188, 2011.

[26] H.P. Mouzakis, I.N. Psycharis, D.Y. Papastamatiou, P.G. Carydis, C. Papantonopoulos, C. Zambas, Experimental investigation of the earthquake response of a model of a marble classical column. *Earthquake Engineering and Structural Dynamics*, **31**, 1681-1698, 2002.

[27] F. Peña, P.B. Lourenço, A. Campos-Costa, Experimental dynamic behavior of free-standing multi-block structures under seismic loadings. *J. Earthq. Eng.,* **12,** 953-979, 2008.

[28] V.A. Drosos, I. Anastasopoulos, Experimental investigation of the seismic response of classical temple columns. *Bulletin of Earthquake Engineering*, **13**(1), 299-310, 2015.

[29] P.D. Spanos, A.S. Koh, Analysis of block random rocking. *Soil Dynamics and Earthquake Engineering*, **5**(3), 178-183, 1986.

[30] I.N. Psycharis, M. Fragiadakis, I. Stefanou, Seismic reliability assessment of classical columns subjected to near‐fault ground motions. *Earthquake Engineering & Structural Dynamics,* **42**(14), 2061-2079, 2013.

[31] E.G. Dimitrakopoulos, T.S. Paraskeva, Dimensionless fragility curves for rocking response to near‐fault excitations. *Earthquake Engineering & Structural Dynamics,* **44**(12), 2015-2033, 2015.

[32] J.E. Padgett, B.G. Nielson, R. DesRoches, Selection of optimal intensity measures in probabilistic seismic demand models of highway bridge portfolios. *Earthquake Engineering & Structural Dynamics*, **37**(5), 711-725, 2008.

[33] C.A. Cornell, F. Jalayer, R.O. Hamburger, D.A. Foutch, Probabilistic basis for 2000 SAC federal emergency management agency steel moment frame guidelines. *Journal of Structural Engineering,* **128**(4), 526-533, 2002.

[34] E.I. Katsanos, A.G. Sextos, G.D. Manolis, Selection of earthquake ground motion records: A state-of-the-art review from a structural engineering perspective. *Soil Dynamics and Earthquake Engineering*, **30**(4), 157-169, 2010.

[35] Pacific Earthquake Engineering Research Centre (PEER). Strong motion database http://ngawest2.berkeley.edu/; 2013.

[36] European Strong-Motion Database. http://www.isesd.hi.is/ESD_Local/frameset.htm; 2008.

[37] S.L. Kramer, *Geotechnical earthquake engineering.* Prentice-Hall, 1996.

[38] E.M. Rathje, N.A. Abrahamson, J.D. Bray, Simplified frequency content estimates of earthquake ground motions. *Journal of Geotechnical and Geoenviromental Engineering,* **124**(2), 150-159, 1998.

[39] N. Makris, C.J. Black, Dimensional analysis of rigid-plastic and elastoplastic structures under pulse-type excitations. J. Eng. Mech. (ASCE), **130**, 1006-1018, 2004.

[40] E. Dimitrakopoulos, A.J. Kappos, N. Makris, Dimensional analysis of yielding and pounding structures for records without distinct pulses. *Soil Dynamics and Earthquake Engineering,* **29**(7), 1170-1180, 2009.

[41] P. Gehl, D.M. Seyedi, J. Douglas, Vector-valued fragility functions for seismic risk evaluation. *Bulletin of Earthquake Engineering,* **11**(2), 365-384, 2013.